6,6′-Bis(*O*-4-pyren-1-yl-ethynylbenzoyl)-α,α-trehalose (aryl-substituted trehalose) activates the NF-κB signaling pathway and is an effective fluorescent probe for cell imaging in HeLa CD4$^+$ cells

Rumiko Saito[1)], Takanobu Nakayama[2)], Kahoko Hashimoto [1), 2)], and Naoko Miyano-Kurosaki [1) ,2) *]

Abstract

Cell imaging is expected to contribute not only to basic life science research but also to clinical diagnosis, treatment, and drug discovery as a method for exploring and interpreting biological phenomena. We have shown that 6,6′-bis(*O*-4-pyren-1-yl-ethynylbenzoyl)-α,α-trehalose (aryl-substituted trehalose) is taken up by HeLa CD4$^+$ cells, a human cervical cancer cell line, and shows bright green luminescence. In this study, we evaluated the effect of aryl-substituted trehalose on HeLa CD4$^+$ cells and its utilization as a cell imaging material. An analysis of the change in intracellular fluorescence of aryl-substituted trehalose over time by fluorescence microscopy revealed uptake by HeLa CD4$^+$ cells and fluorescence signals in the cytoplasm. The number of cells incorporating aryl-substituted trehalose was higher at 48 h than at 24 h after the addition. Aryl-substituted trehalose did not affect cell cycle progression in HeLa CD4$^+$ cells. It was suggested that aryl-substituted trehalose is taken up into cancer cells via glucotransporter in the same way as glucose uptake. Aryl-substituted trehalose is not taken up by normal cells but is specifically taken up by cancer cells, so it may be used for detection of cancer cells.

Keywords：Aryl-substituted trehalose, Cancer cells, Cell imaging material

Received October 5, 2021; accepted November 5, 2021

1) Department of Life and Environmental Sciences, Graduate School of Engineering, Chiba Institute of Technology, 2-17-1 Tsudanuma, Narashino, Chiba 275-0016, Japan

2) Department of Life Sciences, Faculty of Advanced Engineering, Chiba Institute of Technology 2-17-1, Tsudanuma, Narashino, Chiba 275-0016, Japan.

*Corresponding author: Naoko Miyano-Kurosaki, Department of Life and Environmental Sciences, Graduate School of Engineering, Chiba Institute of Technology, 2-17-1 Tsudanuma, Narashino, Chiba 275-0016, Japan

E-mail: kurosaki.naoko@p.chibakoudai.jp

1 Introduction

Bioimaging technology has become an important tool in the field of biomedicine for the multidimensional visualization of biomolecules, cells, tissues, and organisms[1,2]. The visualization of biological phenomena is a focus of disease research and is providing new insights into the etiology of diseases[3,4]. In particular, fluorescence bioimaging, in which fluorescence is imparted to the target substance for visualization, is an indispensable technique in biomedical research[3,5]. For the further development of fluorescence bioimaging technology, it is important to clarify correlations between the molecular structure of imaging materials and optical properties, toxicity, and bioactivity[5].

Fluorescent molecules used in cell imaging include those based on small organic fluorescent molecules and those based on fluorescent proteins, such as green fluorescent protein[6,7]. Imaging with fluorescent proteins requires gene transfer for expression in living cells[8]. Small organic fluorescent substances benefit from their ability to be quickly introduced into all cells simply via extracellular fluid[9].

The design conditions for organic fluorescent small molecule-based imaging materials include a lack of cytotoxicity and high water solubility to ensure *in vivo* compatibility and hydrophobicity for the permeation of cell membranes[10]. Many organic fluorescent molecules are hydrophobic, which can result in various issues, including aggregation and precipitation in extracellular fluid, emphasizing the importance of water solubility.

Against this background, multiple cell imaging techniques in which sugars are complexed with fluorescent molecules have been reported. Hsu *et al.* reported that cell glycans incorporating hyperacetylated alkynyl fucose and *N*-acetylmannosamine by azide-alkyne click chemistry with 3-azido-7-hydroxycoumarin function as fluorescent molecules to label and visualize intracellular complex sugars[11]. Barattucci *et al.* reported that dimethylamino-substituted oligo (phenylene ethynylene) glucosides act as efficient biocompatible fluorescent probes[12,13]. Ribagorda *et al.* found that dimethylamino-oligo glucoside derivatives have photophysical properties, such as high quantum yield, singlet oxygen production, biocompatibility, stability, easy intracellular internalization, and very good responsiveness; they can be utilized as photosensitizers for photodynamic therapy[14]. In addition, Park *et al.* monitored the fluorescence intensity of cells treated with glucosamine-modified silicone rhodamine to efficiently distinguish between cancer cells and normal cells[15]. Therefore, combinations of fluorescent molecules and sugars are expected to be promising fluorescent probes for cell imaging.

Trehalose (α-D-glucopyranosyl-α-D-glucopyranoside) is a disaccharide composed of two glucose molecules linked by an α,α-1,1 bond[16]. Trehalose is widely distributed in nature and is used as an energy source in a broad range of taxa, including bacteria, fungi, insects, plants, and invertebrates[17]. In addition, it is widely used in foods and biomaterials and is attracting attention an excipient for pharmaceuticals. Trehalose has more favorable hydration properties compared with other sugars such as glucose, galactose, and sucrose. Given the need for imaging materials with water solubility for use in living tissues, as well as its hydrophobicity for penetrating the cell membrane and its low cytotoxicity, trehalose is a promising sugar.

We have previously synthesized 6,6′-bis(*O*-4-pyren-1-yl-ethynylbenzoyl)-α,α-trehalose (aryl-substituted trehalose) by TMS protection and selective deprotection of the hydroxy group of trehalose, esterification of the primary hydroxy group, and the Sonogashira coupling reaction[13]. The

aryl-substituted trehalose showed an absorption maximum in the visible region and a high fluorescence quantum yield in diluted THF solutions. It generated strong fluorescent signals. Strong fluorescence was maintained even in a THF/H_2O mixed solvent. We further confirmed that aryl-substituted trehalose could be introduced into HeLa $CD4^+$ cells and used as a green fluorescent probe.

In this study, we evaluated the effects of aryl-substituted trehalose, as a candidate cell imaging material, on HeLa $CD4^+$ cells.

2 Experimental

2.1 Culture conditions and reagents. HeLa $CD4^+$cells and Vero cells were cultured as a monolayer in Dulbecco's Modified Eagle Medium (DMEM; Sigma-Aldrich) supplemented with 10% heat-inactivated fetal bovine serum (Cytiva), 100 units/mL penicillin G, and 100 μg/mL streptomycin (Fujifilm Wako Pure Chemical Corporation). The aryl-substituted trehalose was dissolved in dimethyl sulfoxide (DMSO) and the final concentration of DMSO was 1%.

2.2 Observation of uptake of the aryl-substituted trehalose with a fluorescence microscope. The uptake of the aryl-substituted trehalose by HeLa $CD4^+$ cells and Vero cells was observed using a fluorescence microscope. HeLa $CD4^+$ cells and Vero cells were seeded on 96-well plates (2×10^4 cells/well) for 24 h to allow adherence and were then incubated with aryl-substituted trehalose at concentrations of 0 (1% DMSO) and 9.4 μmol/L for 24 or 48 h. After incubation, nuclear staining was performed using Hoechst33342 (ImmunoChemistry Technologies). Cells were viewed under a fluorescence microscope (Keyence Co.).

2.3 Evaluation of the aryl-substituted trehalose uptake efficiency. Uptake of the aryl-substituted trehalose by HeLa $CD4^+$ cells was observed using a flow cytometer. HeLa $CD4^+$ cells were seeded on 24-well plates (10^5 cells/well) for 24 h to allow adherence and were then incubated with aryl-substituted trehalose at concentrations of 0 (1% DMSO) and 9.4 μmol/L for 24 and 48 h. After they were washed twice with PBS(-), the cells were trypsinized and collected for the measurement of uptake efficiency. Fluorescence was monitored using a flow cytometer (BD Biosciences). Ten thousand events were collected per sample, and the data were analyzed using CellQuest (BD Biosciences).

2.4 Cell proliferation and viability assays. The trypan blue method was used to evaluate the effects of aryl-substituted trehalose on the viability and proliferation of HeLa $CD4^+$ cells and Vero cells. The aryl-substituted trehalose was synthesized and diluted in DMSO. For proliferation and viability assays, 10^5 cells were plated in 24-well plates and treated with aryl-substituted trehalose for 24 and 48 h. After treatment, cells were trypsinized and counted using a TC20 Automated Cell Counter (Bio-Rad Laboratories, Inc.).

2.5 Comparison of glut4 expression in cancer cells and normal cells by adding aryl-substituted trehalose. The expression level of glut4 present on the cell surface was compared to investigate the cell uptake pathway of aryl-substituted trehalose in HeLa $CD4^+$cells and Vero cells. HeLa $CD4^+$ cells were seeded into 24-well plates (10^5 cells/well) for 24 h to allow the cells to grow adherently, followed by incubation with aryl-substituted trehalose at 0 (1% DMSO) and 9.4 μmol/L for 48 h. Cells were stained with PE-binding anti-glut4 antibody (BioLegend) for 15 min, after which glut4 expression levels were measured with a flow cytometer.

2.6 Confirmation of NF-κB and Bcl-X expression by flow cytometry. Cells were incubated with 1% DMSO and 9.4 μmol/L aryl-substituted trehalose for 24 h and 48 h. NF-κB and

Bcl-XL were measured by flow cytometry using PE-conjugated NF-κB and Bcl-X antibodies (BioLegend) along with standard binding buffer. Antibody staining was performed following the manufacturer's recommended protocol.

2.7 Statistical analysis. All data were processed using Microsoft Office Excel (Microsoft). Each experiment was repeated independently at least 3 times, and all results were expressed as mean ± standard deviation (SD). In addition, statistical differences were analyzed by Student's *t*-tests. A *p*-value of less than 0.05 was considered statistically significant.

3 Result

3.1 Aryl-substituted trehalose uptake by HeLa CD4$^+$ cells. Nuclear staining and fluorescence were compared between cells supplemented with 1% DMSO, which solubilizes aryl-substituted trehalose, and cells supplemented with aryl-substituted trehalose. We observed that aryl-substituted trehalose was taken up by HeLa CD4$^+$ cells and Vero cells and then labeled the cytoplasmic compartment (Fig. 1). We have previously confirmed that trehalose at a concentration of 37.5 μmol/L is taken up by cells; in this study, we used the minimum concentration for cellular uptake[13]. Aryl-substituted trehalose was taken up by HeLa CD4$^+$ cells but not by Vero cells. This suggests that aryl-substituted trehalose is taken up by cancer cells but not by normal cells.

3.2 Evaluation of aryl-substituted trehalose uptake in HeLa CD4$^+$cells by flow cytometry. As determined by flow cytometry, the fluorescence intensities of aryl-substituted trehalose in HeLa CD4$^+$ cells at 9.4 μmol/L for 24 and 48 h were

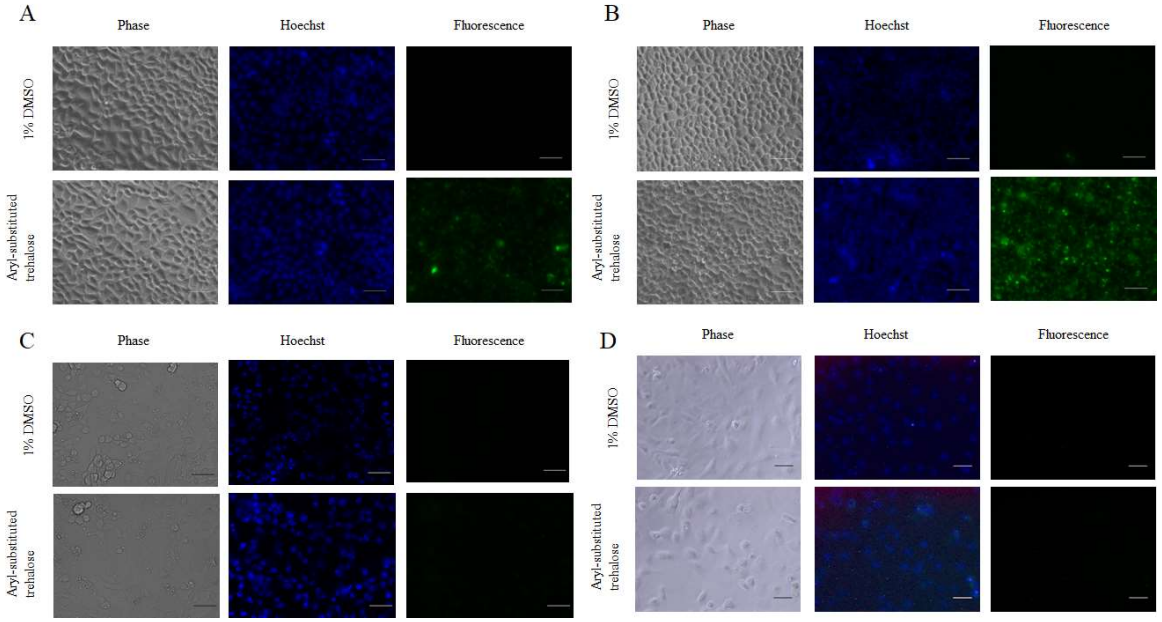

Fig. 1 Analysis of aryl-substituted trehalose uptake by HeLa CD4$^+$cells and Vero cells by fluorescence microscopy. HeLa CD4$^+$cells were incubated with aryl-substituted trehalose or 1% DMSO for 24 h (A) or 48 h (B). Vero cells were incubated with aryl-substituted trehalose or 1% DMSO for 24 h (C) or 48 h (D). From left to right, Phase, Hoechst, and Fluorescence images are shown. Scale bar represents 50 μm.

significantly greater than that in the control by 13% and 22%, respectively (Fig. 2). The fluorescence intensity of aryl-substituted trehalose incorporated into HeLa $CD4^+$ cells increased in a time-dependent manner.

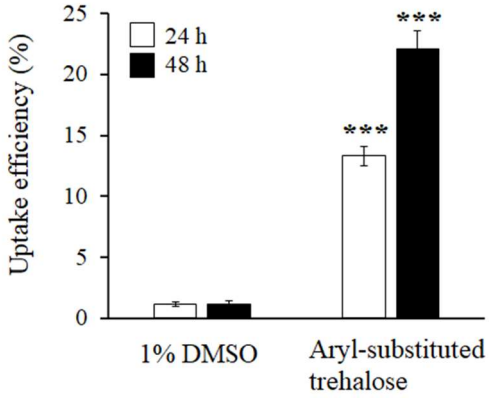

Fig. 2 Flow cytometer analysis of the fluorescence intensity of aryl-substituted trehalose incorporated into HeLa $CD4^+$ cells. Cells were incubated with aryl-substituted trehalose for 24 h (□) or 48 h (■) at concentrations of 9.4 μmol/L and 1% DMSO. Compared with the control, $p < 0.001$ (***). All data are representative of three experiments (±SD).

3.3 Cytotoxicity of aryl-substituted trehalose.

The trypan blue method was used to evaluate the effect of aryl-substituted trehalose on the viability and proliferation of HeLa $CD4^+$ cells and Vero cells. After treatment with aryl-substituted trehalose, cell viability was greater than 90% at both 24 and 48 h. In addition, viability did not differ significantly between treated cells and 1% DMSO (data not shown). There was no difference in cell proliferation between cells that were and were not supplemented with aryl-substituted trehalose after 24 and 48 h (Fig. 3). It was suggested that aryl-substituted trehalose does not affect the proliferative potential of cancer cells and normal cells.

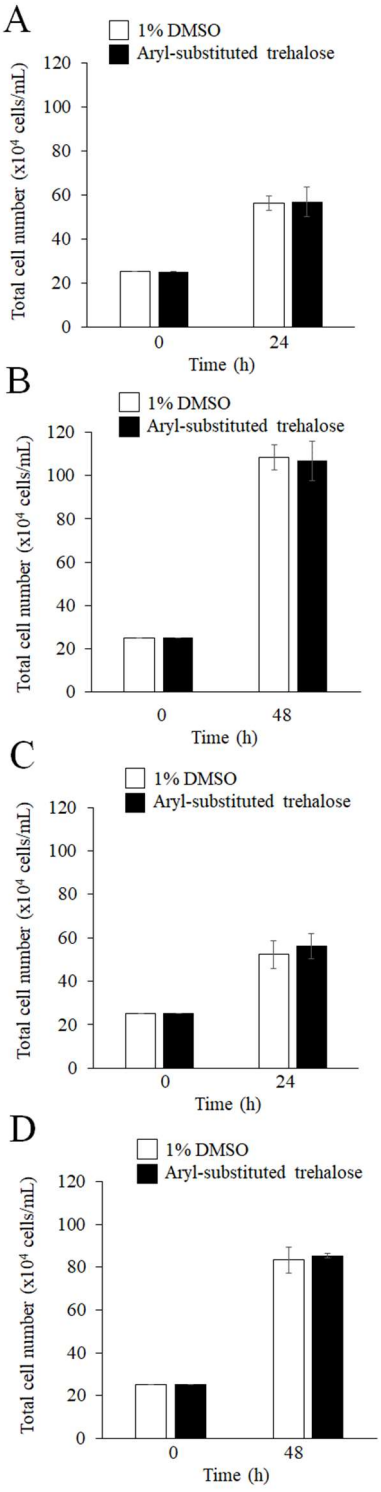

Fig. 3 Proliferation analysis of HeLa $CD4^+$ cells and Vero cells. HeLa $CD4^+$ cells were treated with 1% DMSO and aryl-substituted trehalose for 24 h (A) or 48 h (B). Vero cells were treated with 1% DMSO and aryl-substituted trehalose for 24 h (C) or 48 h (D). All data are representative of three experiments (±SD).

3.4 Intracellular uptake of aryl-substituted trehalose. Cellular glucose uptake is mediated by membrane-bound glucose transporters. The expression level of glut4 present on the cell surface was compared to investigate the cell uptake pathway of aryl-substituted trehalose of HeLa $CD4^+$ cells, which are cancer cells, and Vero cells, which are normal cells. The expression level of glut4 was increased in HeLa $CD4^+$ cells supplemented with aryl-substituted trehalose, but not in Vero cells (Fig. 4). This result suggests that aryl-substituted trehalose is taken up into cells via glut4.

3.5 Expression of factors related to the NF-κB signal transduction pathway. NF-κB expression levels were 14% higher than those in the control for concentrations of 9.4 μmol/L after 24 h and 10% higher after 48 h (Fig. 5A, B). Furthermore, Bcl-XL expression levels were 15% higher than

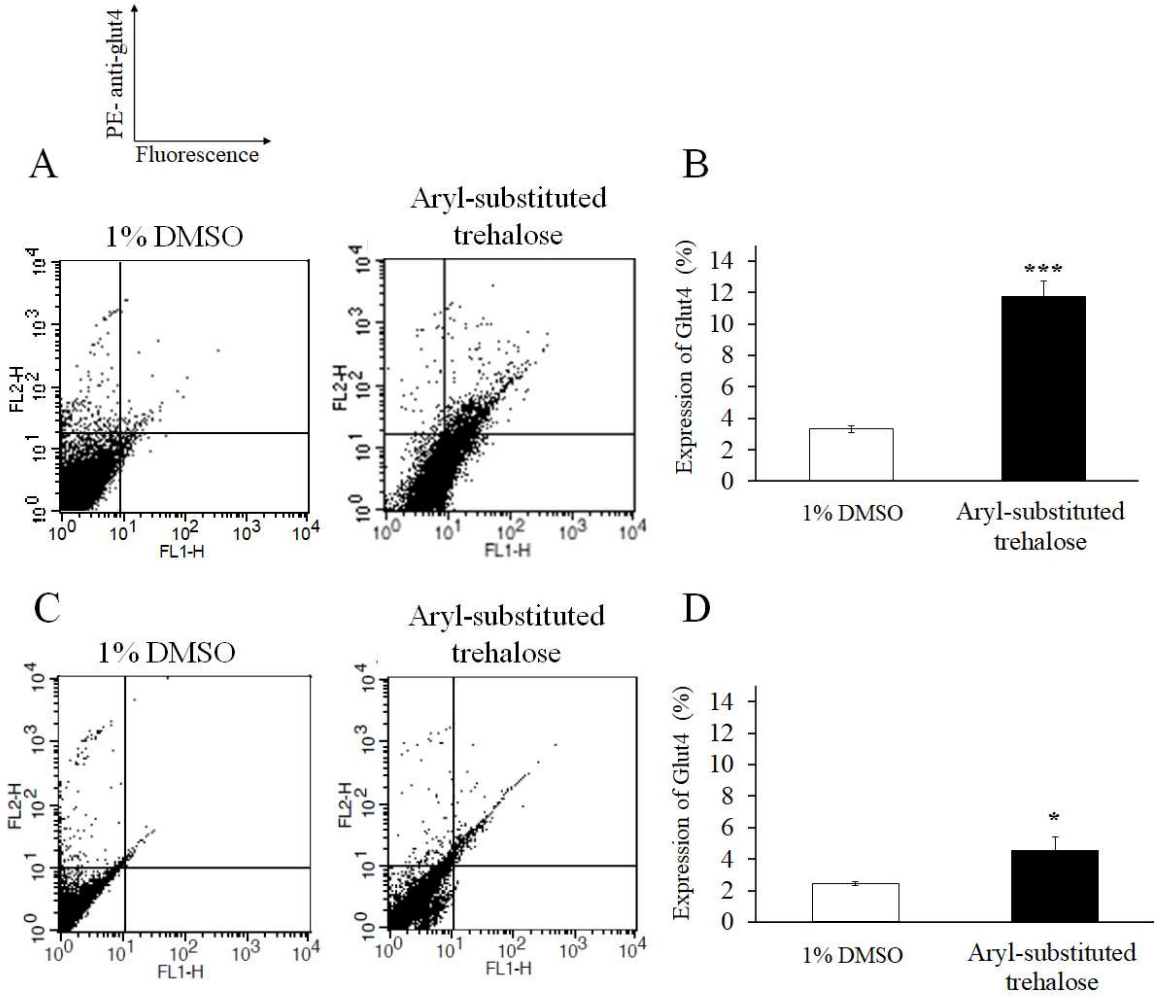

Fig. 4 Comparison of glut4 expression by addition of aryl-substituted trehalose in cancer cells and normal cells. The aryl-substituted trehalose was added to HeLa $CD4^+$ cells (A,B) and Vero cells (C,D). Populations of glut4-positive cells were analyzed using a flow cytometer. Compared to 1% DMSO, $p < 0.05$ (*) or $p < 0.001$ (***). All data are means ± SD of three samples from three independent experiments.

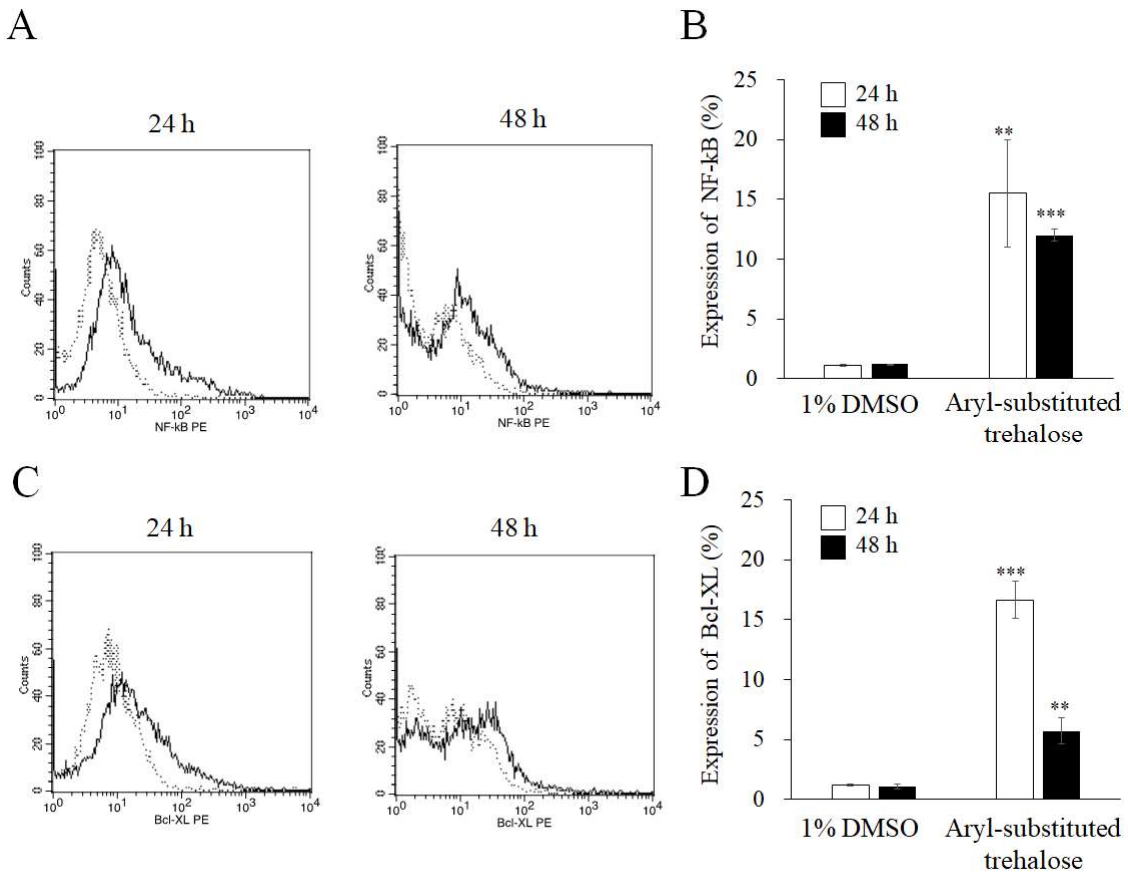

Fig. 5 NF-κB and Bcl-XL expression in response to aryl-substituted trehalose. HeLa $CD4^+$ cells were stained with NF-κB-PE (A,B) or Bcl-XL-PE (C,D) for flow cytometry. (A,C) Representative profile. The solid line and dashed line represent the aryl-substituted trehalose and 1% DMSO, respectively. (B,D) Each bar represents the mean ± SD of three independent experiments ($p < 0.01$ (**) or $p < 0.001$ (***) compared to 1% DMSO).

those in the control for concentrations of 9.4 μmol/L after 24 h and 4% higher after 48 h (Fig. 5C, D). The addition of aryl-substituted trehalose increased the expression of NF-κB signaling pathway-related factors (i.e., NF-κB and Bcl-XL), thereby promoting the survival of HeLa $CD4^+$ cells.

4 Discussion

Cell imaging is expected to contribute to clinical diagnosis, treatment, drug discovery, and life science research as a methodology for exploring and interpreting biological phenomena from a new perspective[18]. One of the design requirements for organic fluorescent small molecule-based imaging materials is a lack of cytotoxicity. Another requirement for the design of an imaging material is good water solubility for adapting to the biological environment and hydrophobicity for penetrating the cell membrane. Therefore, we focused on trehalose, which is a water-soluble sugar. Trehalose has beneficial characteristics for applications as a raw material for processed foods and as an excipient for pharmaceuticals[19]. We successfully synthesized aryl-substituted trehalose, in which trehalose with high hydration ability was combined with a hydrophobic organic fluorescent molecule, for cell imaging. Aryl-substituted trehalose showed efficient time-dependent cellular uptake (Fig. 1).

We verified that aryl-substituted trehalose was taken up by HeLa CD4$^+$ cells and verified its effectiveness as a cell imaging probe. In addition, a quantitative flow cytometry analysis revealed that the fluorescence intensity of aryl-substituted trehalose in HeLa CD4$^+$ cells depends on the treatment duration. HeLa CD4$^+$ cells supplemented with aryl-substituted trehalose did not show morphological changes typical of apoptosis, as evaluated by light microscopy, even 48 h after treatment. During the early stages of apoptosis, cell contraction and enrichment can be observed using a light microscope. Cells show a reduced cell size, dense cytoplasm, densely packed organelles, and pyknosis as a result of chromatin condensation, a morphological feature of apoptosis[20].

NF-κB is a nuclear transcription factor involved in the response to stimuli, such as stress[21]. NF-κB has important roles in inflammatory and immune responses[22]. It also regulates cytokines, which are growth factors in tumor cells, thereby contributing to cell proliferation[23]. In addition, NF-κB activation controls the anti-apoptotic cascade and anti-apoptotic genes, such as genes in the Bcl-2 family[24]. The anti-apoptotic Bcl-2 protein family prevents the physiological destruction of mitochondria, prevents the release of cytochrome c from mitochondria in p53-regulated apoptosis, and suppresses apoptosis[25,26].

Our experimental results showed that the introduction of aryl-substituted trehalose significantly increases the expression levels of NF-κB and Bcl-XL, which act as anti-apoptotic proteins in HeLa CD4$^+$ cells (Fig. 5). These results suggest that the NF-κB signaling pathway is activated in HeLa CD4$^+$ cells treated with aryl-substituted trehalose. Furthermore, the aryl-substituted trehalose-induced increases in the expression of NF-κB and Bcl-XL promoted the maintenance of HeLa CD4$^+$ cell survival. In other words, aryl-substituted trehalose is easily taken up by cells via glut4 and does not affect cell viability and proliferation, so we expect it to be useful as a new cell imaging technology.

In addition, aryl-substituted trehalose did not influence cell proliferation in HeLa CD4$^+$ cells and Vero cells. In this assay, we used HeLa CD4$^+$ cells as a representative cancer cell line and Vero cells as a representative normal cell line. Aryl-substituted trehalose was not taken up by Vero cells but was specifically taken up by HeLa CD4$^+$ cells, suggesting that it may be used for cancer cell detection and drug discovery. We believe that aryl-substituted trehalose will serve as a valuable tool in the treatment of cancer.

Acknowledgments. We would like to thank all of our colleagues for their assistance, especially Ms. K. Kobayashi and Dr. T. Shimasaki, who synthesized the aryl-substituted trehalose (Chiba Institute of Technology).

Conflicts of interest

The authors have no potential conflicts of interest to disclose.

References

1) A. Shibata, *Yakugaku Zasshi*, **2017**, *137*, 1323-1337.
2) J. Cao, B. Zhu, K. Zheng, S. He, L. Meng, J. Song, H. Yang, *Front. Bioeng. Biotechnol*., **2020**, *7*, 487.
3) L. Lu, Z-Y. Wu, X. Li, F. Han, *Acta. Pharmacol. Sin*., **2019**, *40*, 717-723.
4) Y. L. Pak, K. M. K. Swamy, J. Yoon, *Sensors*, **2015**, *15*, 24374-24396.
5) A. S. Boutorine, D. S. Novopashina, O. A. Krasheninina, K. Nozeret, A. G. Venyaminova, *Molecules*, **2013**, *18*, 15357-

15397.

6) Y. Jung, J. Jung, Y. Huh, D. Kim, *J. Anal. Methods. Chem*., **2018**, *14*, 5249765.

7) T. Ebe, *Tanpakushitsu Kakusan Koso*, **2007**, *52*, 1766-1767.

8) S. Subramanian, F. Srienc, *J. Biotechnol.*, **1996**, *49*, 137-151.

9) Y. Shinden, H. Ueo, T. Tobo, A. Gamachi, M. Utou, H. Komatsu, S. Nambara, T. Saito, M. Ueda, H. Hirata, S. Sakimura, Y. Takano, R. Uchi, J. Kurashige, S. Akiyoshi, T. Iguchi, H. Eguchi, K. Sugimachi, Y. Kubota, Y. Kai, K. Shibuta, Y. Kijima, H. Yoshinaka, S. Natsugoe, M. Mori, Y. Maehara, M. Sakabe, M. Kamiya, J. W. Kakareka, T. J. Pohida, P. L. Choyke, H. Kobayashi, H. Ueo, Y. Urano, K. Mimori, *Sci. Rep*., **2016**, *6*, 27525.

10) Y. Urano, M. Kamiya, K. Kanda, T. Ueno, K. Hirose, T. Nagano, *J. Am. Chem. Soc*., **2005**, *127*, 4888-4894.

11) T-L. Hsu, S. R. Hanson, K. Kishikawa, S-K. Wang, M. Sawa, C. H. Wong, *Proc. Natl. Acad. Sci. U. S. A.*, **2007**, *104*, 2614-2619.

12) A. Barattucci, E. Deni, P. Bonaccorsi, M. G. Ceraolo, T. Papalia, A. Santoro, M. T. Sciortino, F. Puntoriero, *J. Org. Chem.*, **2014**, *79*, 5113-5120.

13) K. Kobayashi, R. Saito, K. Udagawa, N. Miyano-Kurosaki, N. Asano, T. Iwanaga, N. Teramoto, T. Shimasaki, M. Shibata, *Euro. J. Org. Chem*., **2018**, *26*, 3444-3453.

14) E. Deni, A. Zamarrón, P. Bonaccorsi, M. C. Carreño, Á. Juarranz, F. Puntoriero, M. T. Sciortino, M. Ribagorda, A. Barattucci, *Eur. J. Med. Chem*., **2016**, *111*, 58-71.

15) A. Jo, J. Sung, S. Lee, H. Nam, H. W. Lee, J. Park, H. M. Kim, E. Kim, S. B. Park, *Bioconjug. Chem*., **2018**, *29*, 3394-3401.

16) S. Ohtake, Y. J. Wang, *J. Pharm. Sci*., **2011**, *100*, 2020-2053.

17) A. Patist, H. Zoerb, *Colloids Surf. B Biointerfaces*, **2005**, *40*, 107-113.

18) T. Haraguchi, *Cell Struct. Funct*., **2002**, *27*, 333-334.

19) C. Colaço, S. Sen, M. Thangavelu, S. Pinder, B. Roser, *Biotechnology (N Y)*, **1992**, *10*, 1007-1011.

20) S. Elmore, *Toxicol. Pathol*., **2007**, *35*, 495-516.

21) J. F. R Kerr, *Toxicology*, **2002**, *181-182*, 471-474.

22) S. Ghosh, M. J. May, E. B. Kopp, *Annu. Rev. Immunol*., **1998**, *16*, 225-260.

23) N. S. Chandel, W. C. Trzyna, D. S. McClintock, P. T. Schumacker, *J. Immunol*., **2000**, *165*, 1013-1021.

24) B. B. Aggarwal, *Cancer Cell*, **2004**, *6*, 203-208.

25) K. S. Ahn, G. Sethi, B. B. Aggarwal, *J. Immunol*., **2007**, *178*, 2507-2516.

26) Y. Dogu, J. Díaz, *Biophys. Chem*., **2009**, *143*, 44-54.